Journal of
Radiation Protection and Research 2023;48(3):144–152
https://doi.org/10.14407/jrpr.2023.00220

pISSN 2508-1888 | eISSN 2466-2461

Color Texture Analysis as a Tool for Quantitative Evaluation of Radiation-Induced Skin Injuries

Sung Young Lee[1], Jin Ho Kim[2,3,4], Ji Hyun Chang[2,3,4], Jong Min Park[2,3,4,5], Chang Heon Choi[2,3,4], Jung-in Kim[2,3,4], So-Yeon Park[3,6]

[1]Gijang Heavy Ion Medical Accelerator, Seoul National University Hospital, Busan, Korea; [2]Department of Radiation Oncology, Seoul National University Hospital, Seoul, Korea; [3]Institute of Radiation Medicine, Seoul National University Medical Research Center, Seoul, Korea; [4]Biomedical Research Institute, Seoul National University Hospital, Seoul, Korea; [5]Department of Radiation Oncology, Seoul National University College of Medicine, Seoul, Korea; [6]Department of Radiation Oncology, Veterans Health Service Medical Center, Seoul, Korea

ABSTRACT

Background: Color texture analysis was applied as a tool for quantitative evaluation of radiation-induced skin injuries.

Materials and Methods: We prospectively selected 20 breast cancer patients who underwent whole-breast radiotherapy after breast-conserving surgery. Color images of skin surfaces for irradiated breasts were obtained by using a mobile skin analyzer. The first skin measurement was performed before the first fraction of radiotherapy, and the subsequent measurement was conducted approximately 10 days after the completion of the entire series of radiotherapy sessions. For comparison, color images of the skin surface for the unirradiated breasts were measured similarly. For each color image, six co-occurrence matrices (red-green [RG], red-blue [RB], and green-blue [GB] from color channels, red [R], green [G], blue [B] from gray channels) can be generated. Four textural features (contrast, correlation, energy, and homogeneity) were calculated for each co-occurrence matrix. Finally, several statistical analyses were used to investigate the performance of the color textural parameters to objectively evaluate the radiation-induced skin damage.

Results and Discussion: For the R channel from the gray channel, the differences in the values between the irradiated and unirradiated skin were larger than those of the G and B channels. In addition, for the RG and RB channels, where R was considered in the color channel, the differences were larger than those in the GB channel. When comparing the relative values between gray and color channels, the 'contrast' values for the RG and RB channels were approximately two times greater than those for the R channel for irradiated skin. In contrast, there were no noticeable differences for unirradiated skin.

Conclusion: The utilization of color texture analysis has shown promising results in evaluating the severity of skin damage caused by radiation. All textural parameters of the RG and RB co-occurrence matrices could be potential indicators of the extent of skin damage caused by radiation.

Keywords: Color Texture Analysis, Quantitative Evaluation, Radiation-Induced Skin Injuries, Skin Surface Images

Original Research

Received July 10, 2023
Revision July 19, 2023
Accepted August 2, 2023

Corresponding author: So-Yeon Park

Department of Radiation Oncology, Veterans Health Service Medical Center, 53 Jinhwangdo-ro 61-gil, Gangdong-gu, Seoul 05368, Korea
E-mail: vsoyounv@gmail.com
https://orcid.org/0000-0001-5643-1457

Introduction

In recent years, the use of ionizing radiation and radioactive materials has rapidly increased and has been used in industry, science, medicine, the military, and many other fields [1–3]. However, this increasing use has been associated with an increase in un-

wanted and uncontrolled exposure to radiation, resulting in several adverse effects on radiation workers and the public. Radiation-induced skin injury is the most common acute adverse effect of radiation exposure and one of the most superficial problems in radiation accidents [4, 5].

Radiotherapy, of which more than 99% is external beam radiotherapy, is a treatment technique in which ionizing radiation penetrates the skin surface and is then delivered to the target volume. Therefore, the exposure of the skin to radiation cannot be avoided because of these characteristics [6]. Radiation-induced skin injury is caused by the depletion of stem cells from the basal layer of the epidermis due to radiation [2, 7, 8]. It can progress from skin erythema and dry desquamation to moist desquamation, and finally to skin ulceration and necrosis. These symptoms of radiation-induced skin injury may severely reduce the quality of life and adversely affect the entire treatment process. Therefore, the severity of radiation-induced skin damage requires an appropriate quantitative evaluation to manage symptoms accordingly.

Subjective and objective methods are available for evaluating the severity of radiation-induced skin injuries. Subjective methods involve the evaluation of symptoms through visual observation and are commonly used in clinical practice. However, this approach varies depending on the investigator. Several institutions have proposed objective methods using various detectors to provide quantitative measures. Yamazaki et al. [9] utilized a color reader and a corneometer to obtain skin color and hydration, respectively. They analyzed the correlation between the severity of radiation-induced skin injury and both L*a*b* skin parameters from the color reader and skin moisture [9]. They scored the skin severity for each patient according to the Common Toxicity Criteria version 3 (CTC v3; National Cancer Institute). For statistical analysis, high correlations were found between CTC v3 score and skin parameters [9]. Park et al. [4] investigated the performance of various color-space parameters obtained from skin images to assess and predict the severity of radiation-induced skin damage. The skin images measured using the skin analysis device were analyzed in various color-space modes, including red, green, blue (RGB); L*a*b*; hue, saturation, value (HSV); and YCbCr. They demonstrated that the red (R) value of the RGB model and the saturation (S) and value (V) values of the HSV model performed better when evaluating acute radiodermatitis [4].

With the rise of advanced image-processing technology and machine learning, texture analysis based on pixels in images is commonly used as an image-processing technique to provide quantitative measures. Lee et al. [10] conducted an objective assessment of radiation-induced skin injuries using texture analysis. However, widely used texture analysis thus far relies solely on a single gray channel in the images. It only analyzes the relationships between gray pixels, which limits its ability to investigate color information in color images. Over the past decade, the field of texture analysis based on gray channels has been extended to color texture analysis [11]. Several color texture analysis algorithms have been developed and proposed for color texture feature extraction [12].

To the best of our knowledge, color texture analysis has not been introduced as a tool for quantitative assessment of the severity of radiation-induced skin injuries. Therefore, in this study, we investigated the performance of texture analysis of color channels to assess severe radiation-induced skin injury and compared it with a single gray channel. By analyzing skin images before and after radiotherapy for irradiated and unirradiated skin, we aimed to find an optimal color textural parameter that can determine the presence of radiation-induced skin damage with high statistical significance.

Materials and Methods

1. Patient Characteristics and Planning

We prospectively selected 20 breast cancer patients who underwent whole-breast radiotherapy after breast-conserving surgery between 2018 and 2020 from a single institution. Patients with breast cancer receiving radiotherapy were enrolled in this study because the treated lesions were close to the skin. This enabled a more precise analysis of the radiation-induced skin injury. All patients were diagnosed with ductal carcinoma in situ and had a median age of 50 years. There were eight left ipsilateral breasts and 12 right-left ipsilateral breasts.

For radiotherapy plans, the planning target volume (PTV) was defined as the entire ipsilateral breast. All patients were prescribed 40.5 Gy in 15 fractions to the PTV. Tangential beam intensity-modulated radiotherapy plans were generated for left breast cancer to reduce the dose volume to the ipsilateral lung and heart. Tangential beam field-in-field plans were generated for right breast cancer. The photon beam energies used in this study were 6 MV or a combination of 6 and 10 MV.

2. Visual Assessment Scoring and Dose Measurement

A visual assessment of the severity of radiation-induced

skin injury was conducted approximately 10 days after the completion of the entire series of radiotherapy sessions ('after RT'). According to the Radiation Therapy Oncology Group (RTOG) scoring system, all patients were independently graded by a specialized radiation oncologist with several years of experience in assessing radiation-induced skin damage.

A calibrated nanoDot optically stimulated luminescent dosimeter (OSLD) system (Landauer Inc.) was used to measure skin doses. In the first fraction of radiotherapy, the OSLDs were located at four measurement points, including the inner, outer, upper, and lower sides of the nipple in the irradiated breast, and skin doses were measured for each patient.

3. Acquisition of Skin Surface Images and Color Texture Analysis

Color images of skin surfaces for irradiated breasts were obtained in white light mode from a mobile skin analyzer (API-100; Aram Huvis) at stable room temperature (25 ± 1 °C) and under stable room light (200 ± 10 lx). The spatial resolution of the device was 1,624 × 1,212 pixels within a measurement area of 1 cm × 1 cm. The first skin measurement was performed before the first fraction of radiotherapy ('before RT'), and the subsequent measurement was conducted ('after RT'). The measurement points were the same as those used for skin dose measurement using the nanoDot OSLDs. For comparison, color images of the skin surface of the unirradiated breasts were measured similarly.

The skin color images (24 bits per pixel) were divided into RGB channels using the source code in MATLAB version R2021a (Mathworks). Each color channel had an integer value ranging from 0 to 255, representing the color intensity.

The color texture analysis used in this study was based on a co-occurrence matrix and Haralick features [11, 13]. We selected displacement (d) of 1 and an angle (θ) of 0° to generate the co-occurrence matrix. For the calculation efficiency, the normalized gray value for each gray image was 64. Using a combination of d and θ, the co-occurrence matrix for each gray channel $M(i,j)$ is defined as follows:

$$M(i,j) = \frac{C(i,j)}{\sum_{i=0}^{i=63}\sum_{i=0}^{i=63} C(i,j)} \quad (1)$$

where $C(i,j)$ is the number of relationships of gray values i and j within a window of d and θ.

Color texture analysis extends Equation (1) by using two different color channels, considering the relationships between i and j separately in each color channel, to calculate the co-occurrence matrix for color texture. For example, $M_{RG}(i,j)$ represents a co-occurrence matrix that considers the relationships between the i value from the R channel and the j value from the green (G) channel. Therefore, for each color image, three matrices (red-green [RG], red-blue [RB], and green-blue [GB]) can be generated, resulting in six matrices, including the individual gray channels (R, G, and blue [B]). Four textural features ('contrast,' 'correlation,' 'energy,' and 'homogeneity') were calculated for each matrix using the MATLAB source code.

4. Statistical Analysis

The Wilcoxon signed-rank test was used to conduct pairwise comparisons of color textural parameter values between irradiated and unirradiated skins for each 'before RT' and 'after RT.' Moreover, the test was also used to investigate whether there was a difference in the value of the color textural parameter between 'before RT' and 'after RT' for each of the breast sides. Spearman's rank correlation coefficients and corresponding p-values were calculated to assess the correlation between skin dose and color texture parameter values. For all statistical tests, statistical significance was considered for p-values less than 0.05. All analyses were conducted using PASW software version 18.0 (SPSS).

Results and Discussion

All patients were graded as having RTOG 1 (faint erythema, dry desquamation, epilation, and diminished sweating) based on the severity of the radiation-induced skin injury. There might be diversity in the severity of radiation-induced skin damage within RTOG 1, which could be a limitation of visual assessment. If the severity could be further subdivided using a quantitative approach, it would allow for more detailed management of radiation-related skin damage [4, 9, 14].

The skin dose values using the calibrated nanoDot OSLDs were 212.4 ± 19.6, 226.8 ± 23.5, 253.1 ± 14.7, and 247.8 ± 18.1 cGy for the inner, outer, upper, and lower sides of the irradiated skin, respectively. We calculated the values of the textural parameters for the gray and color channels, as listed in Table 1. The average values of the other texture features, excluding 'contrast,' were all below 1. When comparing the textural parameter values between the gray and color channels, the 'contrast' values of the color channels were approximately 10 times higher than those of the gray channels. Conversely, the 'correlation,' 'energy,' and 'homogeneity' values

https://doi.org/10.14407/jrpr.2023.00220

Table 1. The Values of Textural Parameters for Gray Channels and Color Channel

Variable	Contrast		Correlation		Energy		Homogeneity	
	Before RT[a]	After RT[b]	Before RT	After RT	Before RT	After RT	Before RT	After RT
Gray channel								
R								
Irradiated	3.814±2.491	5.002±2.583	0.960±0.022	0.954±0.023	0.015±0.005	0.010±0.003	0.639±0.059	0.582±0.055
Unirradiated	4.485±2.743	4.728±2.675	0.957±0.023	0.954±0.021	0.014±0.005	0.013±0.004	0.625±0.061	0.609±0.058
G								
Irradiated	3.157±2.235	3.139±1.843	0.977±0.015	0.978±0.011	0.012±0.003	0.010±0.003	0.661±0.064	0.633±0.055
Unirradiated	3.784±2.576	4.072±2.510	0.974±0.016	0.971±0.015	0.011±0.004	0.010±0.003	0.645±0.065	0.624±0.060
B								
Irradiated	2.550±1.683	2.647±1.338	0.979±0.013	0.979±0.011	0.012±0.003	0.010±0.003	0.671±0.060	0.641±0.053
Unirradiated	2.977±1.900	3.247±1.909	0.977±0.014	0.974±0.014	0.012±0.003	0.011±0.003	0.658±0.061	0.636±0.056
Color channel								
RG								
Irradiated	33.269±25.022	71.380±81.534	0.843±0.051	0.782±0.058	0.004±0.001	0.003±0.001	0.295±0.067	0.239±0.075
Unirradiated	28.678±22.997	31.447±19.385	0.850±0.064	0.849±0.035	0.004±0.001	0.004±0.001	0.310±0.053	0.296±0.057
RB								
Irradiated	47.860±35.000	84.242±81.133	0.798±0.051	0.732±0.054	0.004±0.001	0.003±0.001	0.259±0.073	0.221±0.073
Unirradiated	44.339±32.984	44.765±29.597	0.799±0.056	0.792±0.037	0.004±0.001	0.004±0.001	0.262±0.063	0.263±0.065
GB								
Irradiated	18.664±9.059	20.635±10.589	0.908±0.022	0.902±0.021	0.004±0.001	0.004±0.001	0.344±0.062	0.335±0.058
Unirradiated	21.695±16.590	19.707±8.159	0.907±0.025	0.896±0.024	0.004±0.001	0.004±0.001	0.335±0.071	0.343±0.054

Values are presented as mean±standard deviation.
RT, radiotherapy; R, red; G, green; B, blue.
[a]Before the first fraction of radiotherapy.
[b]Approximately 10 days after the completion of the entire series of radiotherapy sessions.

showed a slightly decreasing trend in the color channel compared with the gray channel.

To consider variations in color, tone, and texture of the skin among individuals and even at different measurement points in one patient, relative values of textural parameters were calculated based on the values on 'before RT,' as presented in Table 2. The relative value was defined as the ratio of the values of the textural parameters for 'after RT' to those for 'before RT.' Regardless of irradiated or unirradiated skins, 'contrast' exhibited an increasing trend on 'after RT' while 'correlation,' 'energy,' and 'homogeneity' generally showed a decreasing trend on 'after RT.' For the R channel from the gray channel, the differences in the values between the irradiated and unirradiated skin were larger than those of the G and B channels. In addition, for the RG and RB channels, where R was considered in the color channel, the differences were larger than those in the GB channel. Red correlates more strongly with radiation-induced skin damage, including skin burns. Fig. 1 shows skin images of both irradiated and unirradiated breasts acquired by the skin analysis device on 'before RT' and 'after RT.' Several institutions have found that the parameters related to the red color, such as a* and R of the RGB mode, increased as radiotherapy progressed, and skin damage due to radiation tended to worsen [4, 9]. Fig. 2. shows skin images of irradiated breasts according to each gray channel to demonstrate the changes in skin texture and tone between 'before RT' and 'after RT.' When the skin was irradiated, all pixel values increased regardless of channels. Among the gray channel, considerable changes in pixel value were found in R channel, compared to other channels.

When comparing the relative values between gray and color channels, the 'contrast' values for the RG and RB channels were approximately two times greater than those for the R channel for irradiated skin. In contrast, there were no noticeable differences for unirradiated skin.

No significant correlations were found between the textural parameters of the irradiated breasts and skin doses. It was observed that the skin dose measurement became challenging when the detectors were positioned on the irregular or curved body surface and between the air and materials, which resulted in considerable uncertainty [15–17]. Therefore, the skin dose values measured in this study may be far from the true values, showing no significant relationship between the textural parameters.

Table 2. Relative Values of Textural Parameters

Variable	Contrast	Correlation	Energy	Homogeneity
Gray channel				
R				
Irradiated	1.794±1.476	0.994±0.028	0.739±0.291	0.916±0.107
Unirradiated	1.351±0.886	0.998±0.028	0.976±0.407	0.980±0.114
G				
Irradiated	1.392±1.235	1.001±0.017	0.877±0.343	0.965±0.108
Unirradiated	1.415±0.918	0.998±0.020	0.981±0.390	0.975±0.120
B				
Irradiated	1.382±1.037	1.000±0.014	0.880±0.337	0.961±0.101
Unirradiated	1.370±0.826	0.997±0.016	0.972±0.358	0.973±0.107
Color channel				
RG				
Irradiated	2.627±2.627	0.930±0.074	0.752±0.227	0.863±0.383
Unirradiated	1.345±0.916	1.009±0.154	1.015±0.298	0.998±0.357
RB				
Irradiated	2.339±2.246	0.920±0.074	0.777±0.231	0.952±0.530
Unirradiated	1.299±0.922	0.997±0.095	1.008±0.279	1.096±0.528
GB				
Irradiated	1.342±0.916	0.993±0.028	0.906±0.288	1.016±0.313
Unirradiated	1.125±0.517	0.988±0.032	0.990±0.251	1.089±0.402

Values are presented as mean±standard deviation.
R, red; G, green; B, blue.

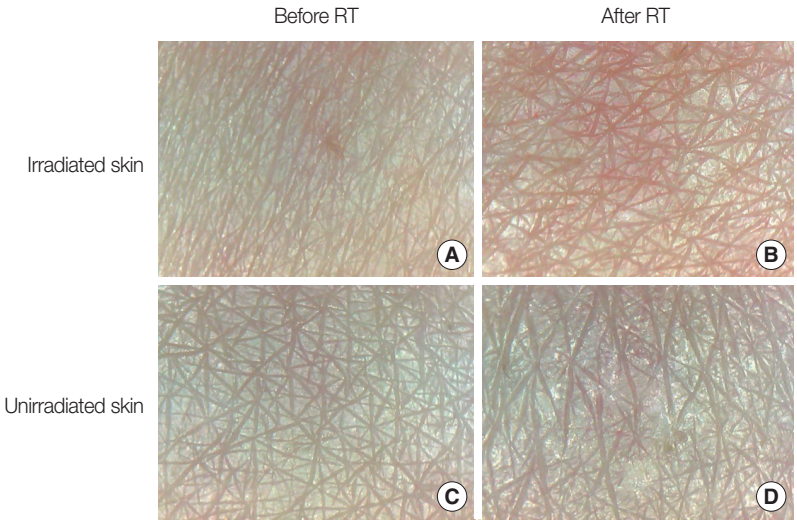

Fig. 1. (A-D) Skin images of both irradiated and unirradiated breasts acquired by the skin analysis device before the first fraction of radiotherapy ('before RT') and approximately 10 days after the completion of the entire series of radiotherapy sessions ('after RT').

The *p*-values of Wilcoxon signed-rank tests that evaluated the differences between 'before RT' and 'after RT' are listed in Table 3. In the statistical analyses, it is expected that there will be no statistically significant difference observed in unirradiated skin, whereas a significant difference is anticipated in irradiated skin. Considering this situation, the 'contrast' and 'correlation' of the R channel showed better performance than those of the other gray channels. For color channels, all textural parameters of the RG and RB channels and 'energy' of GB channel exhibited excellent performance in determining the extent of radiation-induced skin injury between 'before RT' and 'after RT.'

The *p*-values of the Wilcoxon signed-rank tests to evaluate the differences between irradiated and unirradiated skin are listed in Table 4. For these statistical analyses, there should not be a statistically significant difference on 'before RT,'

https://doi.org/10.14407/jrpr.2023.00220

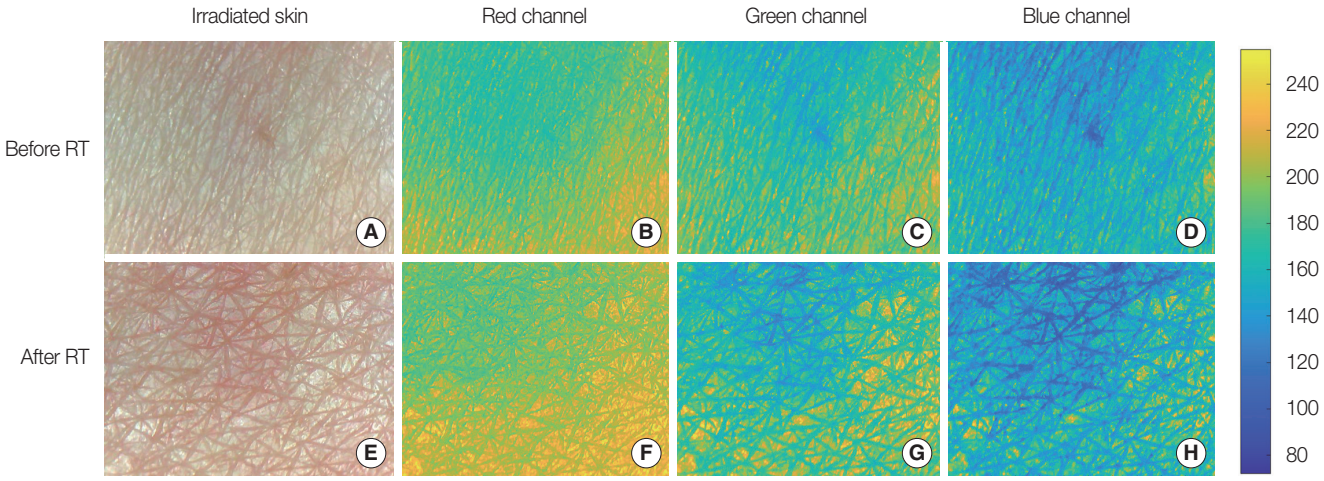

Fig. 2. (A–D) Skin images of irradiated breasts according to each gray channel before the first fraction of radiotherapy ('before RT'). (E–H) Skin images of irradiated breasts according to each gray channel proximately 10 days after the completion of the entire series of radiotherapy sessions ('after RT').

Table 3. Wilcoxon Signed-Rank Tests for Gray and Color Textural Parameters between 'before RT' and 'after RT'

Variable	Contrast	Correlation	Energy	Homogeneity
Gray channel				
R				
Irradiated	<0.001	0.030	<0.001	<0.001
Unirradiated	-	-	0.011	0.017
G				
Irradiated	-	-	<0.001	<0.001
Unirradiated	-	-	0.029	0.005
B				
Irradiated	-	-	<0.001	<0.001
Unirradiated	-	0.017	0.015	0.003
Color channel				
RG				
Irradiated	<0.001	<0.001	<0.001	<0.001
Unirradiated	-	-	-	-
RB				
Irradiated	<0.001	<0.001	<0.001	0.001
Unirradiated	-	-	-	-
GB				
Irradiated	-	0.030	<0.001	-
Unirradiated	-	<0.001	-	-

RT, radiotherapy; R, red; G, green; B, blue.

Table 4. Wilcoxon Signed-Rank Tests for Gray and Color Textural Parameters between Irradiated and Unirradiated Skins

Variable	Contrast	Correlation	Energy	Homogeneity
Gray channel				
R				
Before RT[a]	0.027	-	-	-
After RT[b]	-	-	<0.001	<0.001
G				
Before RT	0.025	-	-	0.043
After RT	0.003	0.001	-	-
B				
Before RT	0.036	0.048	-	-
After RT	0.018	0.001	0.029	-
Color channel				
RG				
Before RT	-	-	-	-
After RT	<0.001	<0.001	<0.001	<0.001
RB				
Before RT	-	-	-	-
After RT	<0.001	<0.001	<0.001	<0.001
GB				
Before RT	-	-	-	-
After RT	-	-	0.009	-

R, red; RT, radiotherapy; G, green; B, blue.
[a]Before the first fraction of radiotherapy.
[b]Approximately 10 days after the completion of the entire series of radiotherapy sessions.

while there should be a statistically significant difference on 'after RT.' Considering this situation, the 'energy' and 'homogeneity' of the R channel and 'energy' of B channel showed better performance than the others. For color channels, all textural parameters of the RG and RB channels and 'energy' of the GB channel exhibited excellent performance in determining the extent of radiation-induced skin injury differences between irradiated and unirradiated skin. However, using two channels for color texture analysis is limited in our study. As introduced by Humeau-Heurtier [11], there are many algorithms to consider all channels at once to calculate textural parameters, expecting to improve performance. In future work, we intend to apply the color texture analysis with all channels at once to evaluate the skin damages by radiation.

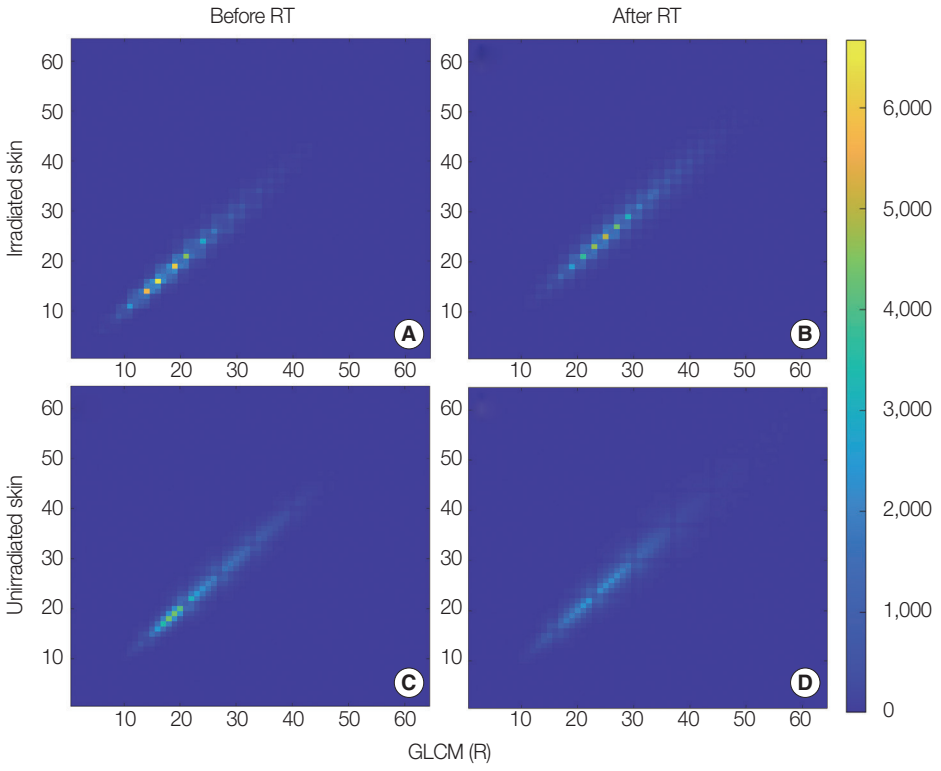

Fig. 3. (A-D) Co-occurrence matrices of red (R) channel for both irradiated and unirradiated skin before the first fraction of radiotherapy ('before RT') and approximately 10 days after the completion of the entire series of radiotherapy sessions ('after RT'). GLCM, gray level co-occurrence matrix.

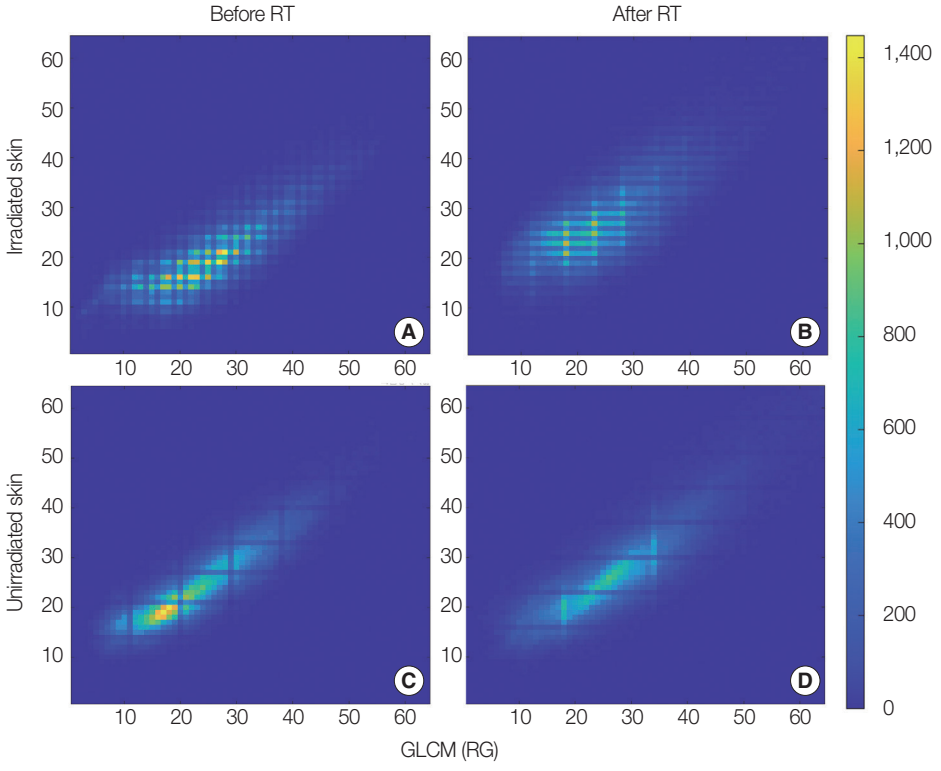

Fig. 4. (A-D) Co-occurrence matrices of red and green (RG) color channel for both irradiated and unirradiated skin before the first fraction of radiotherapy ('before RT') and approximately 10 days after the completion of the entire series of radiotherapy sessions ('after RT'). GLCM, gray level co-occurrence matrix.

https://doi.org/10.14407/jrpr.2023.00220

Consistent with these findings, all textural parameters of RG and RB from the color channels demonstrated excellent performance in determining the presence of skin damage due to radiation. Figs. 3, 4 show the co-occurrence matrices for R and RG in the gray and color channels, respectively. When we considered more than one color channel, large variations in the co-occurrence matrices between 'before RT' and 'after RT' were observed, compared to those of the gray channel. This indicates that considering more than one channel, as opposed to the gray channel, is more appropriate for evaluating radiation-induced skin damage.

Conclusion

In conclusion, this study highlighted the importance of employing color texture analysis to assess radiation-induced skin damage. The utilization of color texture analysis has shown promising results in evaluating the severity of skin damage caused by radiation. All textural parameters of the RG and RB co-occurrence matrices could be potential indicators of the extent of skin damage caused by radiation.

Conflict of Interest

No potential conflict of interest relevant to this article was reported.

Acknowledgements

This study was supported by the National Research Foundation of Korea (NRF) grant funded by the Korea government (MSIT) (No. RS-2023-00253604).

Ethical Statement

All procedures performed in study involving human participants were in accordance with the ethical standards of the institutional and/or national research committee (IRB approval no. D-1810-053-977) and with the 1964 Helsinki declaration and its later amendments or comparable ethical standards. Informed consent was obtained from all individual participants included in the study.

Author Contribution

Conceptualization: Park SY. Methodology: Park JM, Park SY. Formal analysis: Lee SY, Choi CH, Kim J. Funding acquisition: Park SY. Project administration: Lee SY, Kim JH, Park SY. Visualization: Chang JH. Writing - original draft: Lee SY, Park SY. Writing - review & editing: Kim JH. Approval of final manuscript: all authors.

References

1. Wang XJ, Lin S, Kang HF, Dai ZJ, Bai MH, Ma XL, et al. The effect of RHIZOMA COPTIDIS and COPTIS CHINENSIS aqueous extract on radiation-induced skin injury in a rat model. BMC Complement Altern Med. 2013;13:105.
2. Kim JS, Jang H, Bae MJ, Shim S, Jang WS, Lee SJ, et al. Comparison of skin injury induced by β- and γ-irradiation in the minipig model. J Radiat Prot Res. 2017;42(4):189–196.
3. Almuqrin AH, Sayyed MI, Prabhu NS, Kamath SD. Influence of Bi2O3 on mechanical properties and radiation-shielding performance of lithium zinc bismuth silicate glass system using Phys-X software. Materials (Basel). 2022;15(4):1327.
4. Park SY, Kim JH, Chang JH, Park JM, Choi CH, Kim JI. Quantitative evaluation of radiodermatitis following whole-breast radiotherapy with various color space models: a feasibility study. PLoS One. 2022;17(3):e0264925.
5. Delishaj D, D'amico R, Corvi D, De Nobili G, Alghisi A, Colangelo F, et al. Management of grade 3 acute dermatitis with moist desquamation after adjuvant chest wall radiotherapy: a case report. Radiat Oncol J. 2020;38(4):287–290.
6. National Cancer Control Indicators. Radiotherapy treatment activity [Internet]. Cancer Australia; 2017 [cited 2023 Sep 1]. Available from: https://ncci.canceraustralia.gov.au/treatment/radiotherapy-treatment-activity/radiotherapy-treatment-activity
7. Sitton E. Early and late radiation-induced skin alterations. Part II: nursing care of irradiated skin. Oncol Nurs Forum. 1992;19(6):907–912.
8. Cleary JF, Anderson BM, Eickhoff JC, Khuntia D, Fahl WE. Significant suppression of radiation dermatitis in breast cancer patients using a topically applied adrenergic vasoconstrictor. Radiat Oncol. 2017;12(1):201.
9. Yamazaki H, Yoshida K, Kotsuma T, Kuriyama K, Masuda N, Nishimura T, et al. Longitudinal practical measurement of skin color and moisture during and after breast-conserving therapy: influence of neoadjuvant systemic therapy. Jpn J Radiol. 2009;27(8):309–315.
10. Lee CH, Kang CL, Tseng CD, Chou CM, Shieh CS, Lin CH, et al. Photographic image processing to predict radiation dermatitis in breast cancer patients using machine learning algorithms. Int J Mod Phys B. 2021;35(14–16):2140022.
11. Arvis V, Debain C, Berducat M, Benassi A. Generalization of the cooccurrence matrix for colour images: application to colour

texture classification. Image Anal Stereo. 2004;23(1):63–72.
12. Humeau-Heurtier A. Color texture analysis: a survey. IEEE Access. 2022;10:107993–108003.
13. Vrbik I, Van Nest SJ, Meksiarun P, Loeppky J, Brolo A, Lum JJ, et al. Haralick texture feature analysis for quantifying radiation response heterogeneity in murine models observed using Raman spectroscopic mapping. PLoS One. 2019;14(2):e0212225.
14. Kawamura M, Yoshimura M, Asada H, Nakamura M, Matsuo Y, Mizowaki T. A scoring system predicting acute radiation dermatitis in patients with head and neck cancer treated with intensity-modulated radiotherapy. Radiat Oncol. 2019;14(1):14.
15. Kry SF, Smith SA, Weathers R, Stovall M. Skin dose during radiotherapy: a summary and general estimation technique. J Appl Clin Med Phys. 2012;13(3):3734.
16. Dogan N, Glasgow GP. Surface and build-up region dosimetry for obliquely incident intensity modulated radiotherapy 6 MV x rays. Med Phys. 2003;30(12):3091–3096.
17. Court LE, Tishler RB, Allen AM, Xiang H, Makrigiorgos M, Chin L. Experimental evaluation of the accuracy of skin dose calculation for a commercial treatment planning system. J Appl Clin Med Phys. 2008;9(1):29–35.

 https://doi.org/10.14407/jrpr.2023.00220